SIMULTANEOUS SOIL MOISTURE AND CONE INDEX MEASUREMENT

J. W. Hummel, I. S. Ahmad, S. C. Newman, K. A. Sudduth, S. T. Drummond

ABSTRACT. *Soil compaction can restrict root growth and water infiltration, resulting in yield reduction. Maps of yield monitor data aid in visualization of variations in yield, without identifying underlying factors for these variations. Soil penetration resistance can help identify areas where soil physical characteristics are negatively impacting yield. However, penetration resistance is a function of soil moisture content and soil type as well as compaction. A standard penetrometer cone was modified to collect near−infrared reflectance and estimate moisture content. The instrument was tested in the laboratory on a selection of soil types with varying moisture tension levels using stepwise and continuous probe insertions. Soil moisture, dry bulk density, and clay content were significant variables in predicting soil cone index at the lower moisture tension level.*

Keywords. *Sensors, Site−specific, Soil compaction, Soil moisture, Soil strength maps, Tillage.*

Interest in soil compaction, and its effect on crop production and yield, has grown in the latter half of the 20th century with the adoption of large machinery for agricultural crop production. Increased axle loads, and changes in farming operations, have resulted in soil compaction problems, which have been ameliorated by deep plowing to loosen compacted soil (Bengough, 1991). The reduction in compaction has resulted in yield increases, which have been attributed to lowering of mechanical impedance to root growth (Hamblin, 1985). While tillage facilitates burial of crop residue and pulverizes the soil surface, this operation may also enhance water and wind erosion and is an energy−intensive field operation. Researchers have been investigating the basic causes of soil compaction for many years (Davidson, 1965; Morgan et al., 1993; Ngunjuri and Siemens, 1995).

SOIL COMPACTION ASSESSMENT

Penetrometers are typically used to measure soil strength and to identify compacted soil conditions. Commonly used penetrometers include the pocket, cone, and small−diameter friction sleeve cone types (Lowery and Morrison, 2002). The soil cone penetrometer (*ASAE Standards*, 2002b) was initially adopted as an ASAE recommendation in 1968 and was reclassified as an ASAE Standard in 1978. Procedures for use of the soil cone penetrometer have been developed (*ASAE Standards*, 2002a) and indicate that the most desirable moisture content for sample collection is when the soil is near field capacity.

Cone penetrometer resistance, as a means of assessing soil mechanical properties, has been limited by the significant effects of several factors, e.g., soil type, bulk density, and soil moisture. The variability in these factors, both temporally and spatially (horizontally and vertically), has made assessment of the relationship of penetration resistance data to soil compaction difficult during a single sampling period, and virtually impossible across multiple sampling dates.

SITE−SPECIFIC MAPPING OF SOIL COMPACTION

The spatial variability in soil characteristics affects site−specific information, which can be visualized through layers of maps in a Geographic Information System (GIS) (Cambardella and Karlen, 1999). These maps can provide additional information for informed decision−making in formulating best management practices. Simultaneous measurement of soil moisture and soil penetration resistance, in conjunction with maps of soil type, might allow the adjustment of penetration resistance data to compensate for soil type and moisture. This capability would improve soil compaction measurement techniques and the ability to understand the effects of tillage, wheel traffic, and traction on soil productivity.

Several researchers have attempted to measure soil moisture and simultaneously measure soil bulk density and/or soil penetration resistance (Tollner, 1994; Mead et al., 1995; Fulton et al., 1996). In each instance, problems occurred in relating the factors, e.g., a need for a site−specific calibration, differences in calibration among soil types, and/or an inability to predict soil moisture and soil bulk density simultaneously.

Article was submitted for review in January 2003; approved for publication by the Power & Machinery Division of ASAE in March 2004.

Mention of trade names or commercial products in this article is solely for the purpose of providing specific information and does not imply recommendation or endorsement by the USDA or the University of Illinois.

The authors are **John W. Hummel, ASAE Fellow Engineer,** Agricultural Engineer, USDA−ARS Cropping Systems and Water Quality Research Unit, Columbia, Missouri; **Irfan S. Ahmad, ASAE Member Engineer,** Former Post−Doctoral Assistant, and **Symantha C. Newman,** Former Graduate Research Assistant, Department of Agricultural Engineering, University of Illinois at Urbana−Champaign, Urbana, Illinois; and **Kenneth A. Sudduth**, ASAE Member Engineer, Agricultural Engineer, and **Scott T. Drummond,** Computer Specialist, USDA−ARS Cropping Systems and Water Quality Research Unit, Columbia, Missouri. **Corresponding author:** John W. Hummel, 269 Agricultural Engineering Bldg., University of Missouri, Columbia, MO 65211; phone: 573−884−8735; fax: 573−882−1115; e−mail: hummelj@missouri.edu.

A portable soil sensor, which utilized near−infrared (NIR) reflectance, was developed (Sudduth and Hummel, 1993b) and was shown to be capable of predicting soil moisture levels in prepared samples of A−horizon soils with coefficients of determination of over 0.95 and standard errors of 1.5% to 2% d.b. soil moisture (Sudduth and Hummel, 1993c). Additional research (Hummel et al., 2001) showed that the sensor could predict soil moisture in undisturbed soil cores and B−horizon soils, although the sensor−based prediction accuracy was reduced (coefficients of determination of about 0.88 and standard errors of 4.8% to 6.4% d.b. soil moisture.

This article reports on the combination of the portable NIR soil sensor and a cone penetrometer to simultaneously predict soil moisture and measure soil penetration resistance (commonly called "cone index") and laboratory testing of the combined sensor.

Objectives

The overall objective of this research was to design and develop a cone penetrometer system that can be used to remove the effects of soil moisture from soil cone index readings without the need of specific calibrations for different soils. The following sub−objectives were established:

- Design a cone penetrometer for use with the NIR soil sensor to simultaneously determine penetration resistance and moisture content of soil.
- Compare stepwise penetrometer insertion data, including NIR soil moisture data, with the sensor remaining stationary at each depth, to data collected continuously at the standard penetrometer insertion rate.
- Develop a calibration relating soil moisture to NIR reflectance of the soil for a wide range of soil types.
- Evaluate the ability of the soil moisture/soil cone penetrometer sensor to predict soil compaction over a range of soil textures and soil moisture contents.

Soil Moisture/Soil Cone Penetrometer Sensor Design

A standard soil cone penetrometer was modified to accommodate NIR soil moisture sensing through an opening in the cone surface. A stainless steel (SS) cone (base area of 323 mm^2), corresponding to the larger of two standard cone sizes (*ASAE Standards*, 2002b), was bored to accept the terminal end of a fiber−optic bundle fitted with a custom 90˚ mirror tube (Volpi Manufacturing, Auburn, N.Y.) (fig. 1). The window was covered with a 10 mm dia. sapphire plano−convex lens (part 01LSX011, Melles Griot, Irvine, Cal.). The sapphire lens was selected to resist scratching by soil particles, and flush−mounted to minimize soil adherence. The lens replaced about 10% of the SS surface of the cone, but because the frictional characteristics of the lens were similar to those of SS, the effect on cone insertion force was minimized. The hollow steel shaft (15.88 mm O.D. × 9.53 mm I.D.) used to provide a path for the fiber−optic bundle reduced the strength of the shaft by 13%, based on conventional column theory. The reduced strength should have no effect on penetrometer functionality, and minimal effect on durability, since a factor of safety of about 10 appears to exist in the conventional design.

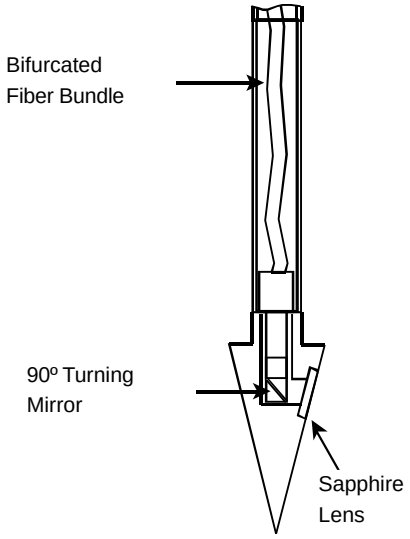

Figure 1. Schematic diagram of the standard soil cone, illustrating the modifications to incorporate a fiber optic bundle and turning mirror to sense soil spectral reflectance.

The NIR soil sensor consisted of a broadband light source (50 W, 12 V quartz halogen automotive−type lamp), circular variable filter (CVF) (Optical Coating Laboratory, Inc., Santa Rosa, Cal.), and a lead sulfide (PbS) photodetector (model OTC−22−53, OptoElectronics, Petaluma, Cal.). The rotating CVF (1600 nm to 3100 nm) sequentially provided monochromatic, chopped light from the broadband source with an apparent bandwidth of 52 nm, and the PbS photodetector measured the energy reflected from the soil surface (Sudduth and Hummel, 1993b). A bifurcated silica−fiber optic bundle was inserted in the system to transmit light energy from the quartz−halogen source to the soil surface and back to the photodetector (Newman and Hummel, 1999). The bifurcated fiber optic cable (Volpi Manufacturing, Auburn, N.Y.) consisted of 328 fibers, with 152 fibers (46%) for transmitting light to the soil surface and 176 fibers (54%) for receiving the reflected light from the soil surface. Combined characteristics of the PbS photodetector and the fiber optics limited the effective sensing range to 1600 nm to 2500 nm. The fiber optic light guide conducted light down the hollow shaft of the penetrometer to the cone, where the 90˚ mirror directed the light through an air gap and the sapphire lens to the soil surface. The light impinged on the soil surrounding the cone, and the reflected portion reentered the cone through the sapphire lens and was transmitted through the second leg of the bifurcated cable to the exit end, which was aligned with the photodetector. The transmission characteristics of the fiber optics and the sapphire lens reduced the signal throughput of the sensor but permitted the photodetector to be positioned above the soil surface.

A reference standard of halon (polytetrafluoroethylene, PTFE) powder was molded to fit the cone. Halon has reflection properties in the ultraviolet, visible, and near−infrared spectral regions that make it a useful standard for diffuse reflectance measurements (Weidner and Hsia, 1981).

Soil Selection and Preparation

Three soils from a group of 30 soils with varying organic matter contents and textures representative of the soils of

Illinois (Worner, 1989) were cleaned, dried, sieved, and stored in 28 cm dia. × 37 cm deep plastic containers (Newman, 1999). The three soils, selected to provide a broad range of soil texture, were: Drummer silty clay loam (fine−silty, mixed, mesic Typic Haplaquolls), Plainfield sandy loam (mixed, mesic Typic Udipsamments), and Shoals silt loam (fine−loamy, mixed, nonacid, mesic Aeric Fluvaquents) (table 1). Soil texture was determined on a composited sample of each soil using the hydrometer method. The moisture contents of the soils were determined using the gravimetric method. Combustion analysis was used to determine organic carbon content of the soils, and organic matter content was estimated by multiplying the organic carbon content by 1.72 (Nelson and Sommers, 1982). The target moisture tension levels for testing were 0.05, 0.1, 0.3, 0.7, and 1.5 MPa, which provided a wide range of moisture contents between field capacity and wilting point. Prior to conducting each set of tests, the volume of soil representing each soil series was divided into five lots, and a different amount of water was added to each lot to adjust the moisture content to approximate the various target moisture tension levels.

Fifteen compacted soil samples in 28 cm dia. plastic containers, one for each soil texture/soil moisture combination, were prepared for each replication. Soil was added to each container in 5 cm lifts, and each lift was compacted by five impacts of a 2.2 kg mass onto the surface of a steel plate placed on the soil surface (Newman, 1999). The target depth was 35 cm, yielding a test depth of approximately 30 cm. The containers were sealed and placed in a cold storage room (5˚C) to minimize moisture loss. Each sample container was emptied, refilled, and recompacted with the same soil for each succeeding replication of each of the two sets of tests.

TEST PROCEDURE

DATA COLLECTION

For the first set of tests (set 1), the sensor was installed on a Tinius−Olsen Electromatic Universal Testing Machine (Newman, 1999), which was powered for at least one hour prior to data collection to stabilize its electrical components. The insertion rate of the combined penetrometer cone/soil moisture sensor was limited to the maximum travel speed of the testing machine (2.5 mm s^{-1}), which was much lower than the 30 mm s^{-1} rate specified in ASAE Standard EP542 (*ASAE Standards*, 2002a). The testing machine was interfaced to an IBM−compatible personal computer (PC) through a General Research Corporation Model T−100 interface connected to a DAS−8 A−D I/O board (Keithley−Metrabyte, Taunton, Mass.). The combined sensor was also interfaced with the PC through the DAS−8 board. The spectrophotometer was powered for at least 30 min prior to data collection to stabilize its light source and electrical components.

A second set of tests (set 2) was conducted to evaluate the sensor while utilizing the ASAE standardized probe insertion speed, and concurrently, to move the sensor onto a platform that, in the future, could be used for field data collection. The combined soil sensor was incorporated into the automated cone penetrometer system on a 12 m wide−span instrumentation carrier (Sudduth et al., 1989). The NIR sensor was mounted on the probe mounting plate using steel shafting and linear ball bearings so that the unit moved vertically in concert with the penetrometer. This mounting minimized flexing of the bifurcated fiber optic bundle that extended from the NIR soil sensor through the 15.9 mm dia. hollow penetrometer shaft to the soil cone.

On the wide−span carrier, the axial compressive force at the connection between the penetrometer shaft and the 51 mm dia. × 760 mm stroke hydraulic cylinder was measured with an 890 N force transducer (model U3SB, BLH Electronics, Inc., Waltham, Mass.) having an output of 3.115 mV V^{-1}. The force transducer output was conditioned to a 0 to 5 V range and input to the data acquisition system through an inline DC transducer amplifier (model S7DC, RDP Electrosense, Pottstown, Pa.) that provided variable excitation, signal amplification, and noise reduction. The force transducer received a regulated 10.0 V excitation, and calibration showed a digital resolution of 0.127 N. The movement of the penetrometer was measured with an incremental shaft encoder (model 70, Litton Industries,

Table 1. Physical characteristics and moisture levels of the soils.

Soil Series and Number[a]	Organic Matter Content[b] (%)	Soil Texture (%)[c]			Moisture Level	Target Moisture Tension (kPa)	Actual Moisture (% d.b.)	
		Sand	Silt	Clay			Set 1	Set 2
Drummer silty clay loam (29)	5.10	12.6	55.9	31.5	5	0.05	24.0	21.4
					4	0.1	21.5	16.5
					3	0.3	16.2	16.2
					2	0.7	13.1	15.8
					1	1.5	8.8	14.3
Plainfield sandy loam (2)	1.73	83.7	12.7	3.6	5	0.05	3.9	7.1
					4	0.1	3.0	4.7
					3	0.3	1.9	4.5
					2	0.7	0.7	3.7
					1	1.5	0.4	2.3
Shoals silt loam (13)	0.61	27.8	59.6	12.6	5	0.05	11.8	19.6
					4	0.1	8.4	12.7
					3	0.3	6.5	12.3
					2	0.7	4.1	10.2
					1	1.5	4.5	5.6

[a] Descriptions of the soil samples and collection sites are included in Worner (1989). The soils sampled by Worner (1989) were numbered for identification.
[b] Organic carbon was determined by combustion analysis, and a multiplier used to obtain organic matter content.
[c] Obtained by the hydrometer method (Worner, 1989).

Chatsworth, Cal.) driven through a rack and pinion. The 1024 pulse/revolution encoder output was input to the personal computer through a counter in the data acquisition system. The digital resolution was 0.099 mm.

For both set 1 and set 2 tests, computer programs were written and used to save spectral reflectance, force, and depth data. A reference scan of the halon reflectance standard was collected prior to each probe insertion. For the stepwise probe insertion, the control program was executed and a scan of the halon reflectance standard was collected, followed by a soil scan (base of soil cone flush with the surface of the soil sample), followed by up to seven scans (the number depended on the depth of soil in the sample container). Stepwise scans were collected at approximately 2 cm and 3 cm depth intervals for the set 1 and set 2 tests, respectively. The reflectance standard scan and the soil scans were stored sequentially, each scan consisting of a sequence of 252 numbers corresponding to known wavelength bands (Sudduth and Hummel, 1993c). Concurrently, force and depth data were stored in another file at a sampling rate of 18.2 Hz. For the continuous probe insertion, the probe was lowered until the base of the soil cone was flush with the surface of the soil sample. A soil scan was collected with the probe stationary, and then a second soil scan was collected as the probe was moving downward through the soil sample at 2.5 mm s^{-1} and 30 mm s^{-1} for the set 1 and set 2 tests, respectively. If multiple spectra were collected, they were stored sequentially in the spectral reflectance data file.

A randomized complete block experimental design was used for both sets of tests with the soil sensor, with replication as the block. Each of the 15 compacted soil samples (3 soils × 5 moisture contents) was transported to the sensor according to the experimental design, and a continuous probe insertion test, a stepwise probe insertion test, and the collection of soil cores for gravimetric moisture analyses were performed. The order of the continuous probe insertion and stepwise probe insertion tests was randomized for each soil/moisture content combination. Probe insertion locations were 10 cm apart, and at least 5 cm from the container wall. During the stepwise probe insertion, spectral reflectance data were collected while the probe was stopped at each depth interval. The number of scans for each stepwise insertion probe ranged from five to seven, depending on the available sampling depth in each soil container. For the continuous probe insertion, spectral reflectance data were collected while the probe was traversing through the soil sample. The spectrophotometer was programmed to sum the output of 64 revolutions of the CVF into each of the wavelength bins, and consequently, required nearly 13 s to collect an individual scan. Thus, scans collected during continuous insertion probes did not occur at one depth but were composites over the depth increment that the probe traversed during the scan data collection.

For the set 1 tests, three soil cores (1.2 cm dia.) were extracted from random locations within each soil container after each pair of penetrometer insertions. The cores were segmented into 2 cm depth intervals and composited for gravimetric moisture analysis (typically 10 to 11 depth increment segments). The disturbance caused by the penetrometer probes and the moisture sampling probes did not permit simultaneous collection of bulk density samples.

For the set 2 tests, the soil core extraction procedure was modified so that bulk density as well as moisture content profiles could be obtained in each soil container. A modified soil coring tube (fig. 2a), equipped with a standard Giddings bit (Giddings Machine Co., Fort Collins, Colo.), was pressed into the soil sample using the electrohydraulic system on the wide−span carrier platform. The resulting core was segmented into 3 cm lengths (figs. 2b, 2c, and 2d), and the mass of each core segment was recorded. Up to seven core segments were collected from each container, depending on the depth of soil. Approximately 20 g of each core segment was weighed and dried at 105°C for 24 hours for gravimetric moisture analysis.

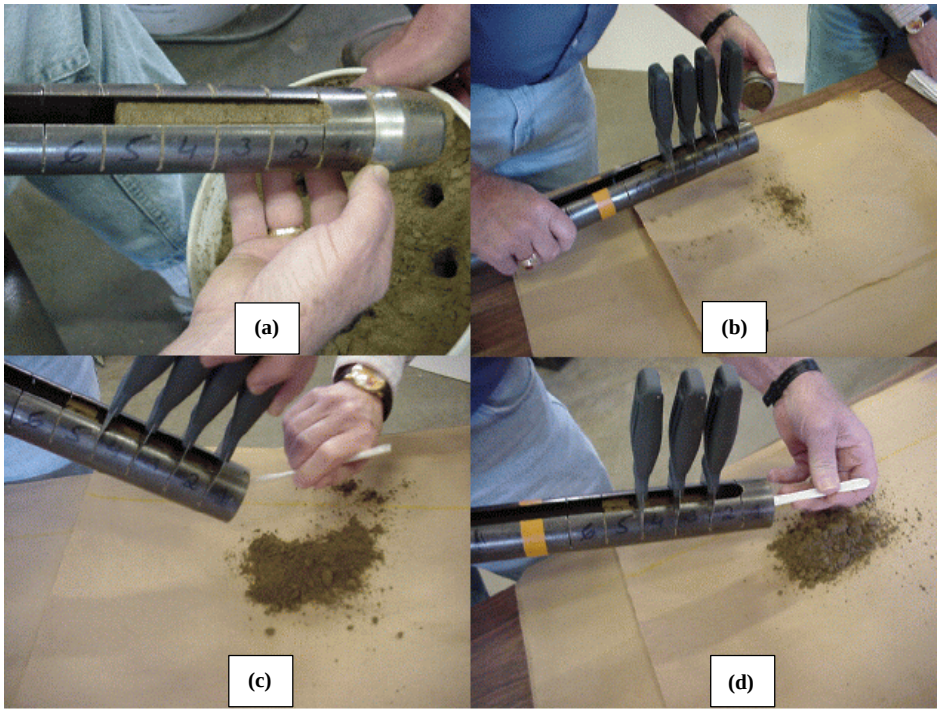

Figure 2. Sample collection technique for obtaining samples at varying depth levels for gravimetric moisture and bulk density analyses (set 2 data).

Data Compilation

In previous research (Sudduth and Hummel, 1993a), a set of coefficients relating soil moisture content with NIR spectral reflectance was developed using Partial Least Squares Regression (PLSR) for the entire group of 30 Illinois soils (Worner, 1989). The PLSR procedure creates factors that are linear combinations of the original reflectance data and determines the maximum number of usable factors without overfitting the data. In this case, there were seven valid factors relating soil moisture and spectral reflectance. Using these factors, coefficients were determined that could be applied to the spectral data to predict soil moisture. The relationship used data (24 bands on a 39.6 nm spacing) from the 1623 nm to 2605 nm portion of the spectrum and required that a sequence of operations be performed to convert raw digitized data obtained from the spectrophotometer to the percent (or decimal) reflectance data needed to estimate soil properties. A compiled C language program was written to calculate a normalized optical density for these wavelength bands by comparison against data obtained with the halon reference standard just prior to the probe insertion, and to apply the set of coefficients to the set 1 data. The form of the equation is:

$$MC = a_o + a_1 \times \log_{10}\frac{ref_1}{dat_1} + ... + a_{24} \times \log_{10}\frac{ref_{24}}{dat_{24}} \qquad (1)$$

where *MC* is soil moisture content (% d.b.), $a_0 \ldots a_{24}$ are the coefficients developed by the PLSR software, and *ref* and *dat* are the digital spectra data from the halon reference standard scan and soil scan, respectively. The subscripts refer to the 39.6 nm spectral bands with center wavelengths from 1640 nm to 2551 nm.k

During post−processing of the set 1 data, a second statistical procedure, stepwise multiple linear regression (SMLR), was employed with a goal of increasing the speed and improving the accuracy of moisture content estimation. The stepwise procedure investigated all of the set 1 spectral scan data and sequentially identified those data that explained the greatest proportion of variance. Another compiled C language program was written for this analysis, and only those terms that were statistically significant at the 5% level were retained. The equation, including those terms that were statistically significant for relating spectral reflectance and soil moisture content, is:

$$MC = a_o + a_1 \times \log_{10}\frac{ref_1}{dat_1} + ... + a_4 \times \log_{10}\frac{ref_4}{dat_4} \qquad (2)$$

where *MC* is soil moisture content (% d.b.), and *ref* and *dat* are the digital spectral data from the halon reference standard scan and soil scan, respectively. The bandpass center wavelengths of the four 6.6 nm bands were 2473 nm, 2309 nm, 2282 nm, and 1742 nm, respectively. The SMLR calibration relating spectral reflectance and soil moisture (eq. 2) was developed using the set 1 data collected for the three soils.

Normalized optical density was also used in developing a relationship between soil moisture and NIR spectral reflectance for the set 2 data. For each of the 265 scans (5 to 7 scans/probe insertion) collected during the 45 stepwise insertion probes (3 soils × 5 moisture contents × 3 replications), decimal reflectance was calculated for all 252 wavelength bands by comparison against data obtained with the halon reference standard just prior to the probe insertion. The scans collected during the continuous insertion probes were not included in the analyses to develop a calibration, since they did not correspond to a specific depth increment and gravimetric moisture content. The decimal reflectance scans were converted to optical density by taking $\log_{10}(1/\text{reflectance})$ for each of the 252 values for each scan. These optical density data were normalized by dividing the optical density value from each wavelength band by the mean of the values from 91 bands, which appeared to be the most stable portion of the wavelength range of the sensor. The normalization procedure appeared to compensate for ambient light contamination of the soil scan taken with the base of the penetrometer cone flush with the soil surface.

Penetrometer depth encoder data were used to determine the depths at which the stepwise insertion NIR reflectance data had been collected, and these data along with continuous probe insertion force data were used in the analyses. The first soil scan, taken with the cone base at the soil surface, was considered to be at zero depth, even though the center of the optical window in the side of the cone was approximately 10.3 mm below the surface.

Soil moisture and dry bulk density data were collected from each soil sample, but the depth intervals did not coincide with the intervals at which NIR reflectance scans were collected. Soil moisture and bulk density at each depth where an NIR reflectance scan had been collected were estimated by straight−line interpolation between the two nearest actual measurements.

Results and Discussion

Electromagnetic interference (EMI) can deteriorate spectral reflectance data quality. During collection of the set 1 data, equipment in a mechanical service room adjacent to the test stand was generating significant EMI. Shielding of the spectrophotometer and cabling was unsuccessful, and test scheduling to avoid the periods of interference was only partially successful. Post−test data processing suggested that signal deterioration due to the electromagnetic interference was a major factor in reducing the soil moisture prediction capability of the dataset. The set 2 data collection, using the wide−span carrier as a platform for the sensor, took place in another building where EMI was not a problem.

Use of a fiber optic bundle for transmitting light to and receiving light from the penetration point attenuated the signal to varying degrees across the entire spectrum (Newman, 1999). Use of a calibration standard compensated for the effect of the diminished output signal. However, above 2400 nm, the output signal was no longer useful, as the magnitude was comparable to background electrical noise.

The laboratory tests were designed to test the functionality of the modified cone penetrometer tip and hollow shaft, and the design performed as expected. Of course, use under controlled conditions in the laboratory did not address the adequacy of the strength and endurance of the design for use in field operations. The sapphire lens was left unmarred, as was expected; however, some soil clung to the upper edge of the lens in the higher moisture samples of soils with higher clay contents.

Laboratory Testing Machine Tests (Set 1 Data)

Moisture Prediction Methods Comparison

The two moisture prediction models (eqs. 1 and 2) were

applied to the set 1 data collected during both the stepwise and continuous probe insertion tests, resulting in four moisture prediction comparisons (table 2). The SAS PROC MEANS statistical analysis procedure (Littell et al., 1991), a comparison of two sets of data, was sequentially used to compare the moisture contents predicted by each of the four moisture prediction methods with the gravimetric moisture contents to determine which prediction procedure most accurately predicted gravimetric moisture content. The procedure was used to test moisture prediction accuracy across the range of soils and moisture contents included in the test. Subsequent applications of the procedure were used to determine if prediction accuracy was better for a particular soil type or soil type/soil moisture combination.

The means of the soil moisture contents predicted by the four prediction procedures were all significantly different from the means of the gravimetric moisture contents (table 2) when all soils and all moisture contents were included in the analysis. Furthermore, many of the means of predicted soil moisture for the individual soils and the soil type/soil moisture combinations were significantly different from the soil moisture means obtained by gravimetric analyses. Overall, soil moisture prediction accuracy with the SMLR method was somewhat better than with the PLSR method for both probe insertion methods. We attribute the improvement to the development and use of regression equation coefficients specifically for the three soils used in the test (SMLR), in contrast with the use of coefficients developed for a larger set of soils (PLSR). The use of coefficients developed with a different sample subset, as was the case for the PLSR prediction, would introduce some error. An additional error source was a fiber optic bundle, with associated signal attenuation, that was not included in the instrument when the data that led to the coefficients used in the PLSR prediction were collected (Sudduth and Hummel, 1991). Finally, the original group of 30 Illinois soils contained more soils of the finer textures, which may have biased the relationship toward these soils. These data indicate that the soil moisture prediction accuracy of the PLSR method was comparable to that of the SMLR method for the Drummer silty clay loam soil, the finer−textured of the three test soils.

Table 2. Prediction of soil moisture from spectral reflectance data collected during set 1 continuous and stepwise probe insertion using stepwise multiple linear regression (SMLR) and partial least squares regression (PLSR) techniques.

Moisture Tension (MPa)	Gravimetric Moisture[a] (% d.b.)	Continuous Probe Insertion[b] SMLR (% d.b.)	Continuous Probe Insertion[b] PLSR (% d.b.)	Stepwise Probe Insertion[b] SMLR (% d.b.)	Stepwise Probe Insertion[b] PLSR (% d.b.)
All soils, all moisture tensions					
	8.4	7.5*	10.4*	7.2*	10.7*
Drummer silty clay loam					
All[c]	17.8	13.7*	15.4*	14.6*	16.7*
0.05	24.0	17.0*	18.2*	18.2*	20.2*
0.1	21.5	17.7*	19.2*	17.5*	19.7*
0.3	16.2	13.7*	14.4*	14.0*	14.8
0.7	13.1	11.9*	12.6	10.2*	14.2
1.5	8.8	9.5	9.5	9.9*	11.2*
Plainfield sandy loam					
All[c]	2.0	2.0	7.3*	2.0	7.0*
0.05	3.9	5.1*	10.7*	5.4*	11.4*
0.1	3.0	−1.0*	12.6*	−2.2*	11.7*
0.3	1.9	2.4	7.3*	3.4*	7.0*
0.7	0.7	2.2*	3.3*	2.0*	2.4*
1.5	0.4	1.0*	2.0*	1.2*	1.9*
Shoals silt loam					
All[c]	6.6	7.3	9.1*	6.3	9.0*
0.05	11.8	8.6*	11.4	18.7*	11.3
0.1	8.4	7.7*	11.5*	7.4*	11.7*
0.3	6.5	6.2	8.3*	5.1*	7.5*
0.7	4.1	10.1*	6.6*	5.6*	7.6*
1.5	4.5	4.4	8.6*	5.5	7.7*

[a] Moisture values presented are means of all samples collected for all depth increments and all replications for each respective soil series and moisture tension.

[b] SMLR = mean SMLR−predicted moisture (% d.b.).
PLSR = mean PLSR−predicted moisture (% d.b.).
Predicted moisture means that are significantly different from the gravimetric mean in the same row at the 5% level, according to the t−test, are indicated with an asterisk (*).

[c] All samples, at all moisture levels for the respective soil series, are included in the grouping.

The SMLR prediction method used spectral reflectance data from only four wavelengths. On the other hand, the PLSR prediction identified seven significant factors, but then used the entire spectrum to develop a soil moisture prediction (eq. 2). Less data to manipulate should make prediction using SMLR more rapid than the PLSR method, which is important in real−time sensing applications. In addition, since data at only four wavelengths are required for the SMLR method, four narrow bandpass filters could be used in place of the CVF in the monochromator. This design alternative would reduce the initial cost, improve serviceability, and extend the life of the instrument since there would be no moving parts.

Moisture prediction capability, as compared to gravimetric moisture methods, was less accurate for these tests than was reported earlier with a similar data collection system (Sudduth and Hummel, 1993a). Considerable reduction in moisture prediction capability was attributed to the intermittent electromagnetic interference that affected some of the soil reflectance spectra. Soil core instability, particularly with the Plainfield loamy sand, may have reduced the accuracy of the set 1 gravimetric data. However, the statistical comparisons of predicted moistures with gravimetric moistures (table 2) do not show reduced prediction accuracy with the Plainfield soil data as compared to the other two soils.

Soil Cone Index Prediction

A soil penetrometer is typically used when soil moisture content is near field capacity (*ASAE Standards*, 2002a), i.e., a soil tension of 0.033 MPa, to assess soil strength. We wanted to evaluate how soil moisture and cone index values could be combined to predict cone index values at the lowest moisture tension (moisture level 5), which was slightly drier than field capacity. A regression analysis was used to relate cone index values at each of the four highest moisture tension levels with the cone index at moisture level 5. Separate analyses were made using the gravimetric, PLSR−predicted, and SMLR−predicted soil moisture values. The analyses were performed over the entire range of soil types and moisture contents, and also within each soil type (table 3). The coefficients of determination (r^2) were used to compare the capability of the resulting relationships to predict cone index at a base or reference moisture level (i.e., moisture level 5). For the entire range of soil types and moisture contents, the following model was obtained for each of the three different methods

of moisture estimation (gravimetric, PLSR predicted, SMLR predicted):

$$CI_5 = a + bCI_x + cCI_x^2 + dM_x + eM_x^2 + fC + gC^2 + hD_x + iD_x^2 \quad (3)$$

where CI_5 is the predicted cone index (kPa) at moisture level 5, *a ...i* are the regression coefficients shown in table 3, CI_x is the cone index (kPa) at moisture level *x*, M_x is the moisture content (%, d.b.), *C* is the clay content (%), and D_x is the dry bulk density (g/cm^3).

High coefficients of determination were obtained for the Shoals and Plainfield soils, irrespective of how the moisture data were obtained. Conversely, low coefficients of determination resulted for the Drummer soil across all three moisture data sets. The coefficients of the variables in the soil cone index prediction equations (eq. 3) for each soil type are also included in table 3.

The contribution of soil bulk density (*D*) to soil cone index prediction was expected to be minimal, since the sample preparation procedure was developed to minimize differences in bulk density of the samples. The coefficients of the bulk density variable were significant in about one−third of the equations (table 3). To better understand the contribution of bulk density to force prediction, the equations were formulated again with bulk density excluded from the list of independent variables. The resulting coefficients of determination changed very little from those obtained with the full set of independent variables (table 3).

These results (table 3) indicate that the prediction of penetration force at moisture level 5, based on penetration force and moisture content measurement under current soil conditions, is as accurate with NIR−predicted moisture content as with gravimetric moisture data. Some improvement in overall prediction capability may be possible if prediction for the heavy, silty clay loam soils, represented in these tests by the Drummer sample, can be raised to the levels shown for the lighter soils. Clay content was a statistically significant variable in the prediction of cone index across all soils, irrespective of the source of soil moisture, when all variables were included (table 3) and remained in the predictive relationships when the bulk density variable was removed, irrespective of whether gravimetric, PLSR− or SMLR−estimated moisture content was used.

Table 3. Coefficients and fit statistics for equations developed for estimating field capacity soil cone index using SMLR and PLSR, and the set 1 data[a] collected at varying soil textures and moisture contents.

			Coefficients of Variables							
	r^2	Intercept (kPa)[b]	Cone Index (kPa)	(Cone Index, kPa)^2	Moisture Content (% d.b.)	(Moisture Content, % d.b.)^2	Clay Content (%)	(Clay Content, %)^2	Bulk Density (g/cm^3)	(Bulk Density, g/cm^3)^2
Gravimetric moisture										
All soils	0.895	−26.80	0.99*	−0.0004*	0.789	0.089	38.6*	−1.37*	53.34	−11.76
Drummer	0.596	301.8*	0.41*	−0.0003*	−18.4*	0.626*	N/A	N/A	−41.68*	13.70*
Plainfield	0.910	−29.41	1.21*	−0.0005*	−9.10	1.326	N/A	N/A	138.0*	−34.90*
Shoals	0.898	211.7*	1.18*	−0.0005*	0.886	−0.057	N/A	N/A	15.13	−11.48
PLSR−estimated moisture										
All soils	0.895	−6.701	1.00*	−0.0004*	−3.83*	0.236*	40.0*	−1.38*	35.18	−7.560
Drummer	0.499	195.8*	0.37*	−0.0003*	−2.34	0.643*	N/A	N/A	−25.21	9.083
Plainfield	0.910	−30.44*	1.21	−0.0005*	−2.50	0.134	N/A	N/A	134.6*	−32.89*
Shoals	0.899	202.7*	1.19*	−0.0005*	4.01	−0.222	N/A	N/A	12.78	−11.83
SMLR−estimated moisture										
All soils	0.896	−10.87	0.99*	−0.0004*	1.33	0.063	37.1*	−1.32*	41.71	−9.092
Drummer	0.505	191.9*	0.36*	−0.0003*	−2.24	0.115	N/A	N/A	−22.85	8.624
Plainfield	0.910	−61.13	1.19*	−0.0005*	−1.90	0.582	N/A	N/A	160.4*	−38.99*
Shoals	0.914	165.8*	1.16*	−0.0005*	8.78*	−0.144	N/A	N/A	90.12	−6.302
Predicted Results with Bulk Density Removed from Model Consideration										
Gravimetric moisture										
All soils	0.894	26.02*	1.00*	−0.0004*	−1.98	0.156	39.3	−1.38		
Drummer	0.579	264.9*	0.38*	−0.0002*	−16.2*	0.562*	N/A	N/A		
Plainfield	0.907	99.21*	1.24*	−0.0006*	20.8*	3.656	N/A	N/A		
Shoals	0.897	200.4	1.18*	−0.0005*	3.24*	−0.108	N/A	N/A		
PLSR−estimated moisture										
All soils	0.895	31.26*	1.00*	−0.0004*	−4.23*	0.246*	39.7*	−1.38*		
Drummer	0.491	185.0*	0.35*	−0.0002*	−2.49	0.108*	N/A	N/A		
Plainfield	0.908	95.87*	1.23*	−0.0006*	−4.48*	0.218	N/A	N/A		
Shoals	0.896	198.5*	1.19*	−0.0005*	3.42	−0.183	N/A	N/A		
SMLR−estimated moisture										
All soils	0.896	31.66*	0.99*	−0.0004*	0.903	0.074	36.9*	−1.32		
Drummer	0.498	182.7*	0.35*	−0.0002*	−2.39	0.119	N/A	N/A		
Plainfield	0.905	85.98*	0.20*	−0.0005*	−1.77	0.534	N/A	N/A		
Shoals	0.914	163.3*	1.17*	−0.0005*	9.30*	−0.156*	N/A	N/A		

[a] Data were collected on a laboratory testing machine, using a probe insertion rate of 2.5 mm s^{-1}.

[b] Form of the equations is shown in equation 3, and an asterisk (*) indicates that the intercept or coefficient is statistically significant at the 5% level, based on the t−test.

The performance of the combined soil moisture/soil cone penetrometer sensor in these tests, even with concerns about EMI, was promising at the reduced insertion speed. Additional testing, with steps taken to eliminate EMI and to operate the probe at the standard probe insertion rate, was scheduled to further evaluate the technique.

WIDE-SPAN CARRIER PLATFORM TESTS (SET 2 DATA)

Calibration of Soil Moisture to NIR Reflectance

For the set 2 data, the relationship of soil moisture to NIR reflectance was established with SMLR, using a 4−fold cross−validation approach. The procedure identified nine reflectance values (eq. 4) that could be used, each contributing significantly to improved calibration and estimation ability. The following equation was used to estimate dry−basis soil moisture content (MC) values at the depths along each probe insertion where an NIR reflectance scan had been collected:

$$MC = -1627.5 + 234.2X_1 + 445.9X_2 - 320.6X_3 + 471.8X_4 + 116.6X_5 + 242.4X_6 + 871.3X_7 - 452.6X_8 + 45.0X_9 \quad (4)$$

where X_1 through X_9 are the reflectance values for a 52 nm bandpass centered at each of the following wavelengths, respectively: 2160, 2108, 2094, 2048, 1883, 1870, 1679, 1626, and 1607 nm. A coefficient of determination (r^2) of 0.896 was obtained, the standard error of calibration (SEC) was 1.97% d.b. moisture, and the standard error of prediction (SEP) was 2.38% d.b. moisture.

A plot of NIR−estimated soil moisture versus gravimetric soil moisture (fig. 3) shows that the ranges of gravimetric soil moisture values for the Drummer, Plainfield, and Shoals soils were approximately 7%, 5%, and 14% d.b., respectively. Selection of 0.033 MPa (field capacity) as the lowest moisture tension level for these tests would have increased these ranges by perhaps 2% d.b., but it would also have caused significant sample preparation problems. Closer matching of actual soil moisture levels during sample preparation with target moistures would have enhanced NIR moisture estimation, especially of the Drummer silty clay loam, where most of the samples exhibited moisture contents in a 7% d.b. range, even though the target moisture range was 18% d.b. The vertically elongated shape of the data cloud for each soil/moisture level combination illustrates the error present in the NIR moisture estimation.

Penetrometer Insertion Force

The penetrometer insertion force data for the stepwise insertion probes were difficult to analyze due to force decreases when probe insertion stopped to collect an NIR reflectance scan. More accurate penetrometer insertion force data were available from the continuous insertion probe, since the insertion rate was constant from the time the probe entered the soil until the maximum penetration depth was achieved. At each of the depths of the stepwise insertion probes, the mean force (from the continuous probe insertion) was calculated for a 1 cm band surrounding the depth of that scan. At the data sampling rate (18.2 Hz) and penetration insertion rate (30 mm s^{-1}), a typical force value was the mean of six data points. These data were merged with the spectral reflectance, soil moisture, and bulk density data at each depth where a reflectance scan was collected during the stepwise probe insertion.

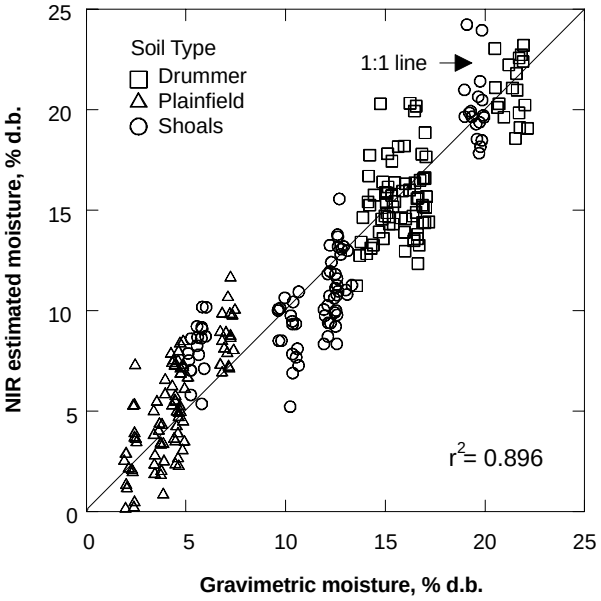

Figure 3. NIR−predicted soil moisture versus gravimetric soil moisture, over all three soils, using the nine−wavelength model (set 2 data).

Soil Cone Index Prediction

As with soil moisture estimation, SMLR was used to develop a relationship to estimate soil cone index at moisture level 5 (table 1) using cone index, soil moisture content, bulk density, and clay content at each of the other four test moisture levels as independent variables. Observation of the force transducer data revealed that force increased with depth within each sample container, even though the samples had been prepared to produce uniform bulk density and moisture content (fig. 4). The graphs also show that cone index values tended to be more scattered at the intermediate moisture levels than at the ends of the moisture range (moisture levels 1 and 5), particularly for the Drummer and Shoals soils.

At the depth of each NIR scan collected during the stepwise probe insertions (moisture levels 1 to 4), a measured soil cone index was calculated using the force data collected during the continuous insertion probes at moisture level 5. A total of 159 usable data points (Drummer = 65, Plainfield = 62, and Shoals = 32), i.e., those scans that had corresponding force data, moisture data, etc., were available for developing a relationship between soil cone indices measured at different soil moisture levels. Since both gravimetric soil moisture and NIR−predicted soil moisture values were available for each data point, analyses were conducted using data from both soil moisture sources (table 4). For both analyses, possible linear and quadratic relationships of any of the independent variables with the dependent variable were investigated. Similar equations, in terms of coefficients of determination, standard errors, and significant variables, were obtained when including data for all three soils in the SMLR analysis to predict soil cone index at a moisture level approaching field capacity, irrespective of the source of the soil moisture data. However, the coefficient of the moisture variable was no longer significant when gravimetric soil moisture was replaced with NIR−estimated soil moisture. Evidently the

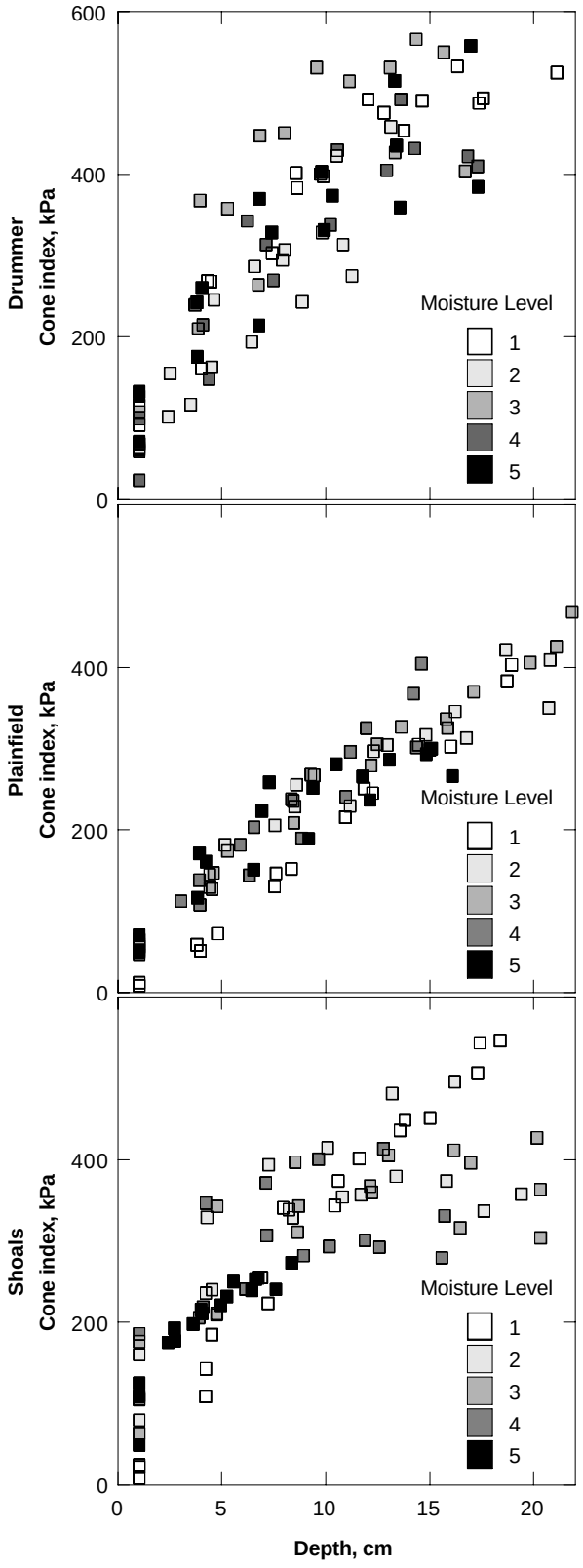

Figure 4. Cone index versus depth for each of the three soils investigated, and their corresponding gravimetric moisture levels (set 2 data).

errors associated with moisture estimation (SEP = 2.38%) were sufficiently large to affect the relationship. When the data were grouped and analyzed by soil series, lower predictive capability was exhibited with the Shoals silt loam soil (table 4). This reduced predictive capability may have occurred because less test soil in the container, for this soil, limited the insertion depth of the probes. Because of the reduced insertion depth, fewer data points (and only low force values) were obtained for the Shoals soil as compared to the other two soils included in this study. The coefficient of the moisture content variable was not statistically significant for any data sets in which both bulk density and NIR−estimated moisture were used as variables.

The effect of soil moisture on soil cone index is evident (fig. 5) when predicted cone index at moisture level 5 (approaching field capacity) is plotted versus measured soil cone index at moisture levels 1 to 4 (the lower moisture levels). A plot of predicted soil cone index versus measured soil cone index (fig. 6) illustrates how the range of cone index values is affected by soil texture. The ability to predict cone index (r^2 = 0.869) at one soil moisture using multivariable data, including gravimetric soil moisture, collected under other conditions, is also evident. The plot (fig. 7) resulting from the same model as fig. 6, but with NIR−estimated soil moisture instead of gravimetric soil moisture, provided similar prediction accuracy (r^2 = 0.856).

A plot of predicted soil cone index versus measured soil cone index using the model for Plainfield loamy sand (fig. 8) illustrates the excellent prediction accuracy (r^2 = 0.918; table 4) of this model for the loamy sand soil. Conversely, the Plainfield model provides poor prediction of soil cone index for the other two soils, also illustrated in figure 8. Obviously, more accurate cone index predictions were possible within a single soil texture class.

Soil bulk density, both as linear and quadratic terms, was a significant variable when cone index prediction was attempted using data for all three soils. Removal of soil bulk density as a variable in the SMLR analyses (table 4) resulted in slight increases in the standard errors as compared to those obtained with the full set of variables. Soil moisture was a significant variable in this model, irrespective of whether gravimetric or NIR−predicted soil moisture was used when predicting soil cone index across all three soils.

Clay content was a statistically significant variable in the prediction of cone index across all soils, irrespective of the source of soil moisture values, when all variables were included (table 4) and remained in both predictive relationships when the bulk density variable was removed. This result is similar to that obtained in the laboratory testing machine tests (table 3). Results from both tests indicate that some information on soil type and/or texture, whether by onboard analysis or the use of prior mapping and the Global Positioning System (GPS) to georeference position on the landscape, would be desirable to improve spatial and temporal cone index prediction in an in−field situation. This information could also be used to select the appropriate calibration curve for each soil type, if different calibration curves for different soil textural classes improve the cone index prediction accuracy.

Statistical analyses were conducted to evaluate the impact of using additional variables to predict soil cone index at one moisture level, e.g., field capacity, using data collected at other moisture levels (table 5). The coefficients of variables and other statistical information from table 4 for the “all soils” relationships (both with and without bulk density) have been included for comparison purposes. In addition, analyses are reported with clay content removed from the statistical analysis, and analyses using only cone index at varying soil

Table 4. Coefficients and fit statistics for equations developed for estimating field capacity soil cone index using SMLR and set 2 data[a] collected at varying soil textures and moisture contents.

				Coefficients of SMLR Variables							
	Standard Error (kPa)	r^2	Intercept (kPa)[b]	Cone Index (kPa)	(Cone Index, kPa)^2	Moisture Content (% d.b.)	(Moisture Content, % d.b.)^2	Clay Content (%)	(Clay Content, %)^2	Bulk Density (g/cm^3)	(Bulk Density, g/cm^3)^2
Gravimetric moisture											
All soils	41.94	0.869	−493.60	0.981	−0.00058	−9.418		6.779		693.2	−221.1
Drummer	52.29	0.832	−79.20	1.053	−0.00068			N/A	N/A		110.57
Plainfield	24.32	0.926	357.09	1.504	−0.00183	−131.375	15.189	N/A	N/A		−41.80
Shoals	39.49	0.743	152.38	0.597		−9.308		N/A	N/A		
NIR−estimated moisture											
All soils	43.93	0.856	−624.6	0.906	−0.00051			4.384		737.2	−200.8
Drummer	52.33	0.832	−79.18	1.053	−0.00068			N/A	N/A		110.57
Plainfield	31.90	0.866	20.31	1.255	−0.00138			N/A	N/A		
Shoals	43.09	0.693	−152.8	0.560				N/A	N/A		154.8
Predicted Results with Bulk Density Removed from Model Consideration											
Gravimetric moisture											
All soils	43.05	0.861	56.30	0.978	−0.00051	−12.228		6.134			
Drummer	54.50	0.814	39.62	1.103	−0.00068			N/A	N/A		
Plainfield	25.33	0.918	232.32	1.367	−0.00157	−115.197	13.882	N/A	N/A		
Shoals	39.49	0.743	152.38	0.597		−9.308		N/A	N/A		
NIR−estimated moisture											
All soils	45.92	0.838	87.95	0.684		−5.729			0.0899		
Drummer	54.50	0.814	39.62	1.103	−0.00068			N/A	N/A		
Plainfield	31.90	0.866	20.31	1.255	−0.00138			N/A	N/A		
Shoals	47.36	0.616	78.49	0.508				N/A	N/A		

[a] Data were collected on a wide−span carrier platform, using the specified probe insertion rate of 30 mm s^{-1} (*ASAE Standards*, 2002a).

[b] Form of the equations is shown in equation 3, and only coefficients of variables that are statistically significant at the 5% level, based on the t−test, are shown.

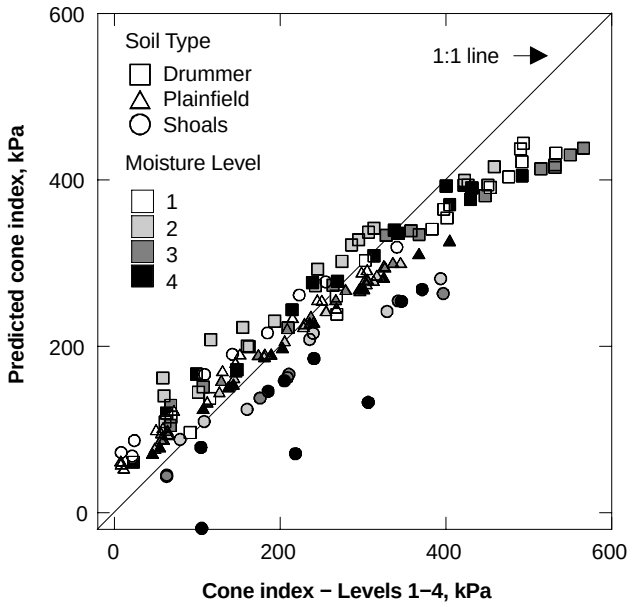

Figure 5. Predicted cone index at moisture level 5 versus measured cone index at moisture levels 1 to 4, using the model derived from all soils and gravimetric moisture (set 2 data).

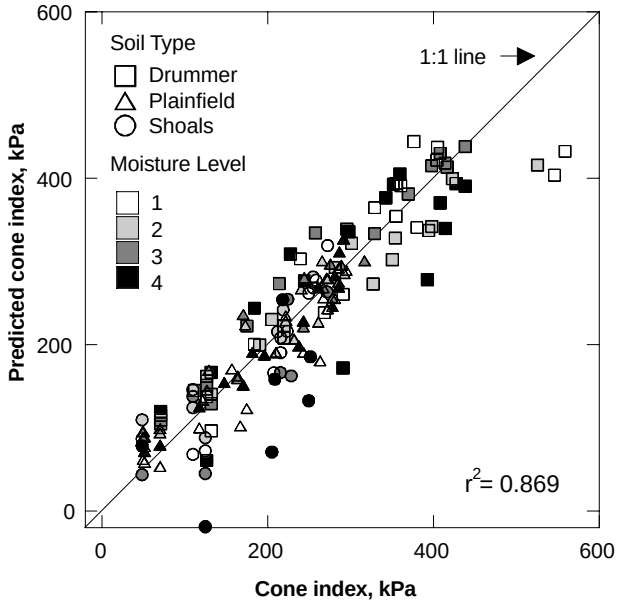

Figure 6. Predicted cone index at moisture level 5 versus measured cone index at moisture level 5, using the model derived from all soils and gravimetric moisture (set 2 data).

moisture levels to estimate cone index at moisture level 5 were also conducted. Considering the relationships developed using gravimetric moisture (table 5), soil bulk density provided little improvement in the correlation coefficient. Soil texture, represented by clay content, had a greater impact on both standard error and correlation coefficient than did soil bulk density. This result is underscored by the very different intercepts and coefficients among the three soil series (which mainly differ in soil texture) shown in table 4. When bulk density was removed from model consideration for the individual soil types and NIR−estimated moisture was included (table 4), the coefficients of the moisture content variables were no longer significant. Thus, these relationships show that soil moisture and texture information are

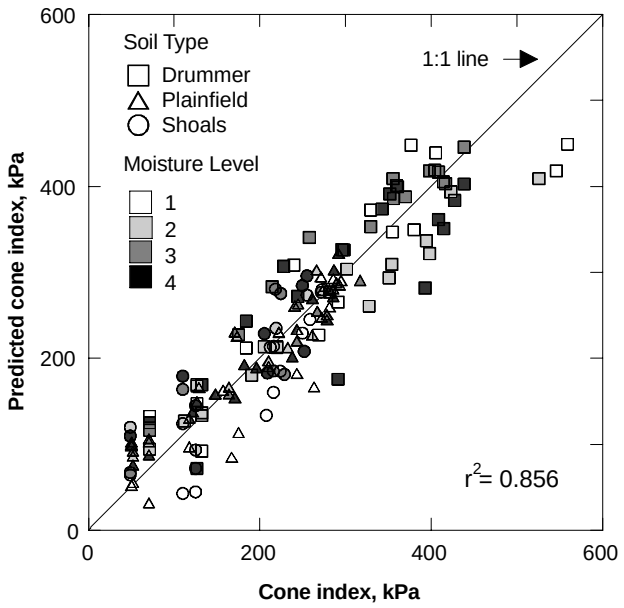

Figure 7. Predicted cone index at moisture level 5 versus cone index at moisture level 5, using the model derived from all soils and NIR estimated moisture (set 2 data).

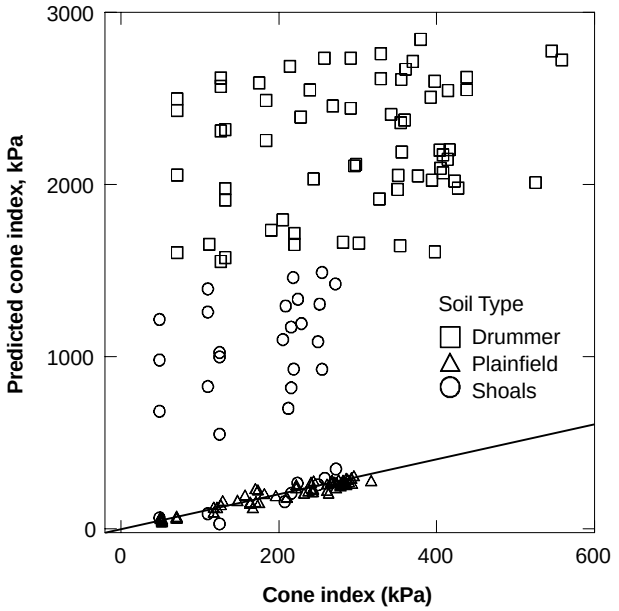

Figure 8. Predicted cone index at moisture level 5 versus measured cone index at moisture level 5, using the model derived from Plainfield sandy loam soil and gravimetric moisture.

Table 5. Overall comparison of coefficients and fit statistics for equations developed for estimating field capacity soil cone index using SMLR and set 2 data[a] collected at varying soil textures and moisture contents.

				Coefficients of Variables[b]							
	Standard Error (kPa)	r^2	Intercept (kPa)	Cone Index (kPa)	(Cone Index, kPa)^2	Moisture Content (% d.b.)	(Moisture Content, % d.b.)^2	Clay Content (%)[c]	(Clay Content, %)^2	Bulk Density (g/cm^3)	(Bulk Density, g/cm^3)^2
All soils, gravimetric moisture											
All variables	41.94	0.869	−493.60	0.981	−0.00058	−9.418		6.779		693.2	−221.1
w/o density	43.05	0.861	56.30	0.978	−0.00051	−12.228		6.134			
w/o density and clay	47.94	0.827	93.39	0.916	−0.00042	−16.62	0.914				
w/o density, clay and moisture	49.90	0.809	59.81	0.728							
All soils, NIR−estimated moisture											
All variables	43.93	0.856	−624.6	0.906	−0.00051			4.384		737.2	−200.8
w/o density	45.92	0.838	87.95	0.684		−5.729			0.0899		
w/o density and clay	49.90	0.809	59.81	0.728	[d]		[d]				
w/o density, clay and moisture	49.90	0.809	59.81	0.728							

[a] Data were collected on a wide−span carrier platform, using the specified probe insertion rate of 30 mm s^{-1} (*ASAE Standards*, 2002a).
[b] Form of the equations is shown in equation 3, and only coefficients of variables that are statistically significant at the 5% level, based on the t−test, are shown.
[c] The clay content value was obtained through textural analysis.
[d] The coefficients of (cone index)^2 and (moisture content)^2 were very close to being significant (α = 0.092 and 0.081, respectively).

useful in adjusting soil cone index values, but that the accuracy of the on−the−go moisture estimation technique needs to be increased.

Cone index prediction on the wide−span carrier platform used predicted soil moisture from spectral reflectance data obtained during the stepwise insertion probes in conjunction with force measurement data obtained during the continuous insertion probe. This was a sequential, rather than simultaneous, measurement technique, which was necessary because the CVF monochromator in the NIR spectrophotometer results in a sequential, rather than simultaneous, collection of spectral reflectance data. For real−time field application of this technique, a new sensor design providing instantaneous, simultaneous spectral reflectance data will be required.

CONCLUSIONS

The standard penetrometer cone, modified to incorporate fiber optics to transfer light to an NIR soil sensor, provided data to simultaneously predict moisture content and determine penetrometer resistance. Limited testing of the cone and shaft design revealed no major design problems.

Stepwise and continuous (2.5 mm s^{-1}) penetrometer probes of soil samples, conducted with the penetrometer cone/soil moisture sensor on a laboratory testing machine, showed that the combined sensor was able to estimate soil moisture content, although the prediction accuracy was low. Soil moisture prediction was more accurate when using a relationship between moisture and reflectance developed by SMLR using the data collected in these tests than when a

previously developed relationship based on PLSR analysis of a broader range of soils was used, even though the latter approach utilized data from the full NIR spectra. Reduced signal amplitude due to fiber optic signal attenuation and increased random noise due to EMI from adjacent mechanical equipment required a new calibration to improve prediction capabilities. However, cone index prediction at a standard soil moisture level was as accurate using NIR−predicted soil moisture as with gravimetric moisture.

Subsequent tests utilized stepwise and continuous (30 mm s^{-1}) penetrometer probes of soil samples conducted on a wide−span carrier data collection platform where EMI was not a factor. NIR spectral reflectance data collected from the stepwise insertion probes were able to predict soil moisture, using stepwise multiple linear regression (SMLR), with a coefficient of determination of 0.896. The standard error of calibration (SEC) was 1.97% d.b. moisture, and the standard error of prediction (SEP) was 2.38% d.b. moisture. The cone index prediction equation for the data over the entire range of soil type/moisture content at the standard probe insertion speed yielded r^2 values of 0.83 or higher. Gravimetric soil moisture content was a significant variable, indicating that accurate simultaneous measurement of soil moisture would be useful to improve soil cone index prediction. Separate calibrations of soil moisture versus spectral reflectance for different textural classes appears to improve moisture prediction accuracy and could be implemented by using GPS to locate field sampling sites on previously obtained textural maps. A new sensor design will be needed for collection of instantaneous, simultaneous spectral reflectance and penetration resistance data.

ACKNOWLEDGEMENTS

The contributions of Christopher Lesiak, Robert Funk, Stuart Birrell, Dennis King, and Teresa Holman to the completion of these studies are gratefully acknowledged.

REFERENCES

ASAE Standards. 2002a. EP542: Procedures for using and reporting data obtained with the soil cone penetrometer. St. Joseph, Mich.: ASAE.

*ASAE Standard.*2002b. S313.2: Soil cone penetrometer. St. Joseph, Mich.: ASAE.

Bengough, A. G. 1991. The penetrometer in relation to mechanical resistance to root growth. In*S oil Analysis: Physical Methods*, 431−435. K. A. Smith and C. E. Mullins, eds. New York, N.Y.: Marcel Dekker.

Cambardella, C. A., and D. L. Karlen. 1999. Spatial analysis of soil parameters. *Precision Agric.* 1(1): 5−14.

Davidson, D. T. 1965. Penetrometer measurement. In *Methods of Soil Analysis: Part 1*, 472−484. C. A. Black, ed. Madison, Wisc.: ASA−CSSA−SSSA.

Fulton, J. P., L. G. Wells, S. A. Shearer, and R. I. Barnhisel. 1996. Spatial variation of soil physical properties: A precursor to precision tillage. ASAE Paper No. 961002. St. Joseph, Mich.: ASAE.

Hamblin, A. P. 1985. The influence of soil structure on water movement, crop growth, and water uptake. *Adv. Agron.*38: 95−158.

Hummel, J. W., K. A. Sudduth, and S. E. Hollinger. 2001. Soil moisture and organic matter prediction of surface and subsurface soils using an NIR soil sensor. *Comp. Elect. in Agric.* 32(2): 149−165.

Littell, R. C., R. J. Freund, and P. C. Spector. 1991. *SAS System for Linear Models*. 3rd ed. Cary, N.C.: SAS Institute, Inc.

Lowery, B., and J. E. Morrison. 2002. Soil penetrometers and penetrability. In *Methods of Soil Analysis: Part 4. Physical Methods*, 363−388. 1st ed. J. H. Dane and C. G. Topp, eds. Madison, Wisc.: ASA−CSSA−SSSA.

Mead, R. M., J. E. Ayars, and J. Liu. 1995. Evaluating the influence of soil texture, bulk density, and soil water salinity on a capacitance probe calibration. ASAE Paper No. 953264. St. Joseph, Mich.: ASAE.

Morgan, M., R. G. Holmes, and R. K. Wood. 1993. A system for measuring soil physical properties in the field. *Soil Tillage Research* 26(1): 301−325.

Nelson, D. W., and L. E. Sommers. 1982. Total carbon, organic carbon, and organic matter. In *Methods of Soil Analysis: Part 2. Chemical and Microbiological Properties*, 539−579. N. R. Page, ed. Madison, Wisc.: ASA−SSSA.

Newman, S. C. 1999. Soil penetration resistance with soil moisture correction. Unpublished MS thesis. Urbana, Ill.: Department of Agricultural Engineering, University of Illinois at Urbana−Champaign.

Newman, S. C., and J. W. Hummel. 1999. Soil penetration resistance with moisture correction. ASAE Paper No. 993028. St. Joseph, Mich.: ASAE.

Ngunjuri, G. M. N., and J. C. Siemens. 1995. Wheel traffic effects on corn growth. *Trans. ASAE* 38(3): 691−699.

Sudduth, K. A., and J. W. Hummel. 1991. Evaluation of reflectance methods for soil organic matter sensing. *Trans. ASAE* 34(4): 1900−09.

Sudduth, K. A., and J. W. Hummel. 1993a. Near−infrared spectrophotometry for soil property sensing. In *Proc. SPIE Conference on Optics in Agriculture and Forestry*: Vol. 1836, 14−25. J. A. DeShazer and G. E. Meyer, eds. Bellingham, Wash.: SPIE.

Sudduth, K. A., and J. W. Hummel. 1993b. Portable, near−infrared spectrophotometer for rapid soil analysis. *Trans. ASAE* 36(1): 185−193.

Sudduth, K. A., and J. W. Hummel. 1993c. Soil organic matter, CEC, and moisture sensing with a portable NIR spectrophotometer. *Trans. ASAE* 36(6): 1571−1582.

Sudduth, K. A., J. W. Hummel, and M. A. Levan. 1989. Widespan vehicle for data collection in tillage research. *Trans. ASAE* 32(2): 367−372.

Tollner, E. W. 1994. Measurement of density and water content in soils with x−ray linescan and x−ray computed tomography. *Trans. ASAE* 37(6): 1741−1748.

Weidner, V. R., and J. J. Hsia. 1981. Reflection properties of pressed polytetrafluorethylene powder. *J. Optical Soc. America* 71(7): 856−861.

Worner, C. R. 1989. Design and construction of a portable spectrophotometer for real−time analysis of soil reflectance properties. Unpublished MS thesis. Urbana, Ill.: Department of Agricultural Engineering, University of Illinois at Urbana−Champaign.